J Electroceram (2009) 23:548–553
DOI 10.1007/s10832-008-9532-0

Effect of a hydrogen ratio in electrical and optical properties of hydrogenated Al-doped ZnO films

S. J. Tark · Y.-W. Ok · M. G. Kang · H. J. Lim · W. M. Kim · D. Kim

Received: 31 May 2007 / Accepted: 18 June 2008 / Published online: 19 July 2008
© Springer Science + Business Media, LLC 2008

Abstract This study examined the effect of the hydrogen ratio on the electrical and optical properties of hydrogenated Al-doped zinc oxide (AZO) thin films deposited by rf magnetron sputtering using a ceramic target (98 wt% ZnO, 2 wt% Al_2O_3). Various AZO films on glass were prepared by changing the $H_2/(Ar+H_2)$ ratio at room temperature. The AZO/H films showed a lower resistivity and a higher carrier concentration and mobility than the AZO films. However, the resistivity and mobility of the AZO/H films increased and decreased with increasing H_2 flow ratio, respectively. As a result, the AZO/H films grown with 2% H_2 addition showed excellent electrical properties with a resistivity of 4.98×10^{4} Ωcm. The UV-measurements showed that the optical transmission of the AZO/H films was >85% in the visible range with a wide optical band gap. In addition, the effect of H_2 flow ratio on the structure and composition of hydrogenated AZO thin films have also been studied.

Keywords ZnO · Al doping · Hydrogenated · rf magnetron sputtering

S. J. Tark · Y.-W. Ok · M. G. Kang · H. J. Lim · D. Kim (✉)
Department of Materials Science and Engineering,
Korea University,
Anam-dong, Seongbuk-gu,
Seoul 137-713, South Korea
e-mail: solar@korea.ac.kr

S. J. Tark
e-mail: tarkwind@korea.ac.kr

W. M. Kim
Division of Materials, Thin Film Materials Research Center,
Korea Institute of Science and Technology,
Seoul 130-650, South Korea

1 Introduction

Transparent conducting zinc oxide films have attracted considerable attention on account of their good electrical and optical properties in combination with their abundance in nature and non-toxicity. They feature a wide band gap non-stoichiometric n-type semiconductor with a low resistivity and high transmittance in the visible region. Therefore, transparent conducting zinc oxide films are promising alternatives to ITO [1]. ZnO is used as a transparent conductor material in solar cells and is a promising material for transparent transistors, which can be used in a variety of consumer products [2–4].

The conductivity of the ZnO films can be changed by several orders of magnitude by doping with Al, Ga or F or by creating oxygen vacancies. These films are typically prepared by magnetron sputtering, chemical vapor deposition and sol-gel process [5–6]. Among these methods, sputtering is widely used in industrial products because the high quality films produced i.e. high density, strong adhesion, high hardness, etc., can be obtained at low substrate temperatures with relatively uniform film thickness over a large area. The microstructure and properties of the sputtered films are strongly dependent on the process parameters, such as the partial pressure of oxygen and sputtering power, substrate temperature [7], etc. Therefore, precise control of each parameter is essential for obtaining high quality sputtered films.

Recently, there has been particular interest in the properties of hydrogen in ZnO because density function theory and total energy calculations predict that it should be a shallow donor [8–11]. The generally observed n-type conductivity can be explained by the presence of residual hydrogen from the growth ambient, rather than to native

defects such as Zn interstitials or O vacancies. Nevertheless, there are few reports on the influence of hydrogen on the electrical and optical properties of AZO grown by magnetron sputtering. The role of hydrogen in the growth process of magnetron sputtered AZO films is not completely understood.

This paper reports the effects of different Ar+H_2 ambient on the structural, electrical and optical properties of AZO films deposited on glass substrates by rf magnetron sputtering. The ZnO/Al films obtained with the addition of hydrogen to the sputtering gas were characterized. The improvement in conductivity produced by the action of H_2 and the structural modifications of the deposited films were examined.

2 Experimental details

ZnO/Al films, approximately 250–300 nm thick were deposited on glass substrates (Corning Eagle 2000) by radio frequency (rf) magnetron sputtering. A sintered ceramic ZnO target (98 wt%) with Al_2O_3 (2 wt%) was used. The glass substrates were sequentially cleaned ultrasonically in acetone, alcohol and de-ionized water, and finally dried with nitrogen gas. The distance between the target and substrate was approximately 50 mm. The rf magnetron working power and deposition time was 50 W and 60 min, respectively. The sputtering system was pumped down to a base pressure of 1×10^{-6} Torr using a turbo molecular pump. The working pressure was approximately 3 mTorr with the H_2 and Ar mixture gas being flowed into the reaction chamber. The sputtering processes were carried out in both Ar and Ar+H_2 plasma. In particular, a series of ZnO/Al films were deposited changing the H_2/(Ar+H_2) ratio from 0% to 10%. The H_2/Ar ratio was controlled using mass flow controllers. The substrate was not heated intentionally and was rotated at a constant speed of 5 rpm during sputtering. The effects H_2 ambient on the properties of AZO films were examined by depositing the samples at different H_2 flow ratios of 0%, 2%, 5%, 7% and 10% with other conditions remaining unchanged.

The electrical resistivity, Hall mobility, and carrier concentration was determined from the Hall-effect measurement equipment using a Van der Pauw method. The changes in the orientation and surface morphology were examined by X-ray diffraction (XRD, Cu K_α wavelength= 1.540562 Å, θ–2θ scan mode) and atomic force microscopy (AFM). The optical transmission and reflection spectra were obtained using a UV-visible spectrophotometer (Perkin Elmer, Lamda35) at wavelengths ranging of 250–1,100 nm. A specially made hot probe system (HPS) was used to obtain the thermal record of the AZO thin films.

3 Results and discussions

Figure 1 shows the XRD patterns of the AZO films deposited at different H_2 flow ratios. All the AZO films showed a (002) diffraction peak, which is an indication of the polycrystalline structure with a preferential orientation of the *c*-axis perpendicular to the substrate. The (002) plane in ZnO crystals had the lowest surface energy so that the continuous films tended to transform into the (002) orientation films in order to minimize the surface energy. The (002) peak of the AZO film prepared without H_2 was situated at 2θ=34.2°. Since the radius of Al^{3+} ion is smaller than Zn^{2+} ion [12], substitution of Al^{3+} ion to the Zn^{2+} site would lead to lattice shrinkage. The lattice expansion observed in non-hydrogenated AZO film suggests that the Al^{3+} ions reside in both the substitutional and interstitial sites [13]. With increasing H_2, the position of the (002) peaks shifted toward lower diffraction angle, indicating a fairly large relaxation as was predicted in the first principle calculation [11].

The grain size of the AZO films at different H_2 flow ratios were evaluated from the full-width at half-maximum (FWHM) of the (002) peak using Scherrer's formula [14]. The calculated FWHM and grain size of the AZO films were plotted as a function of the H_2 flow ratio in Fig. 2(a). The estimated crystallite size decreased from 24.88 to 18.44 nm with increasing H_2 flow ratio from 0 to 10%. Figure 2(b) shows the H_2 flow ratio dependence of the root mean-square (RMS) roughness for the AZO films. As the H_2 flow ratio was increased from 0 to 10%, the RMS roughness decreased from 6.93 to 2.41 nm, respectively. The decrease in surface roughness can cause improvements in the electrical and optical properties [15]. However, as

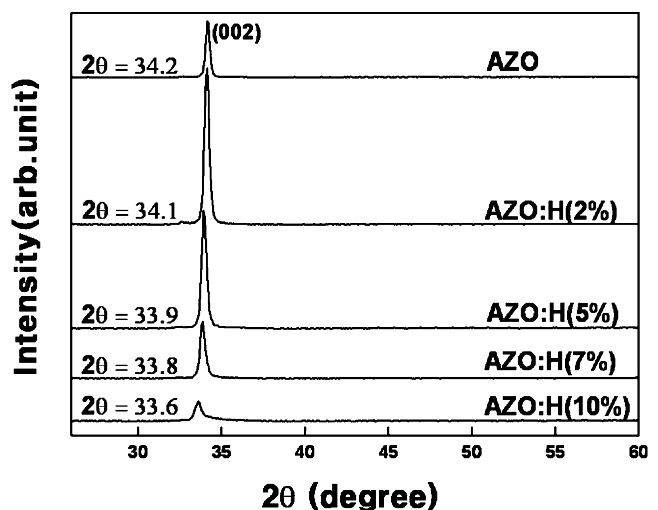

Fig. 1 XRD diffraction pattern of Al doped ZnO and hydrogenated AZO films at different H_2 flow ratios

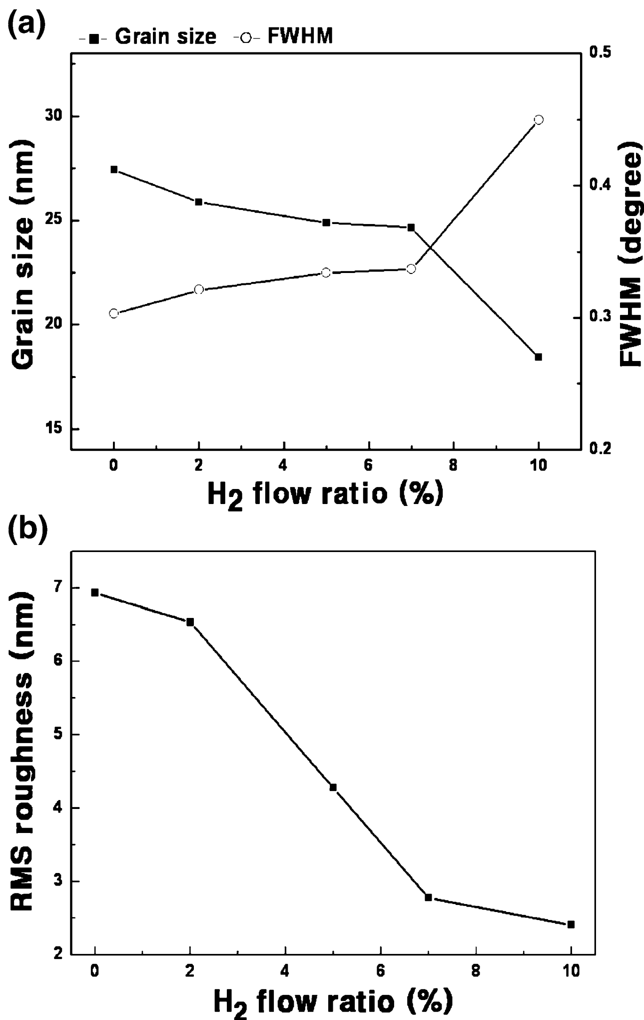

Fig. 2 (**a**) FWHM and grain size of the hydrogenated AZO films prepared at different H_2 flow ratio. (**b**) RMS roughness of hydrogenated AZO films prepare at different H_2 flow ratio

shown below, these differences in the RMS roughness do not appear to have a significant effect on the electrical and optical properties of the films. Therefore, together with the XRD results, hydrogen appears to play a favorable role in the improvement in the electrical and optical properties of the ZnO/Al films.

The calculated compressive stresses and *c*-axis lattice parameter of these films are plotted in Fig. 3, respectively. Based on the XRD data, the lattice parameter of *c* has been estimated in the range of 5.242 to 5.325 Å, which is larger than the American Society for Testing and Materials value of 5.200 Å for bulk ZnO, and from that the stress in the film has been calculated. The calculation of the film stress is based on the biaxial strain model [16]. The lattice parameter *c* for hexagonal close packed ZnO is equal to twice the interplanar spacing *d* of the basal planes, measured from the position of the (002) peak using the Bragg equation. Film strain ϵ_z along the *c*-axis is then given by $\epsilon_z=(c-c_0)/c_0$, where c_0 is the strain-free lattice parameter measured from a ZnO powder sample. The biaxial film stress s is related to the measured *c*-axis strain by the modulus of elasticity:

$$\sigma = [(2C_{13} - (C_{11}+C_{12})(C_{33}/C_{13}))]\,\epsilon_z \tag{1}$$

where C_{ij} are elastic stiffness constants for ZnO. By using the following tabulated values for C_{ij} [17], C_{11}=209.7 GPa, C_{12}=121.1 GPa, C_{33}=210.9 GPa, and C_{13}=105.1 GPa, it is calculated that a tensile *c*-axis strain is proportional to a compressive biaxial stress, and is given by

$$\sigma = -453.6 \times 10^9\,\epsilon_z. \tag{2}$$

As the H_2 flow ratio increase from 0% to 10%, compressive stress increase from 3.17 to 10.42 Gpa.

From these results AZO thin films, as compared with ZnO films, were stretched vertically by compressive stress. Therefore, an increase in the d-spacing of (0002) led (002) peak position shift toward lower angles with an increase in the H_2 flow ratio. Stress increase is consistently accompanied by a decrease in grain size [18].

Figure 4(a) shows the resistivity, carrier concentration and mobility of the AZO films deposited at various H_2 flow ratios. The electrical resistivity and carrier concentration of the as-grown AZO film were 2.02×10^3 Ωcm and 5.35×10^{20} cm3, respectively. The resistivity firstly decreased significantly with increasing H_2 flow ratio to 2% and then increased slightly with further increase of H_2 flow ratio. The minimum resistivity of 4.98×10^3 Ωcm was monitored AZO/H film deposited at H_2 flow ratio of 2%, which was caused by significant increase of the carrier concentration

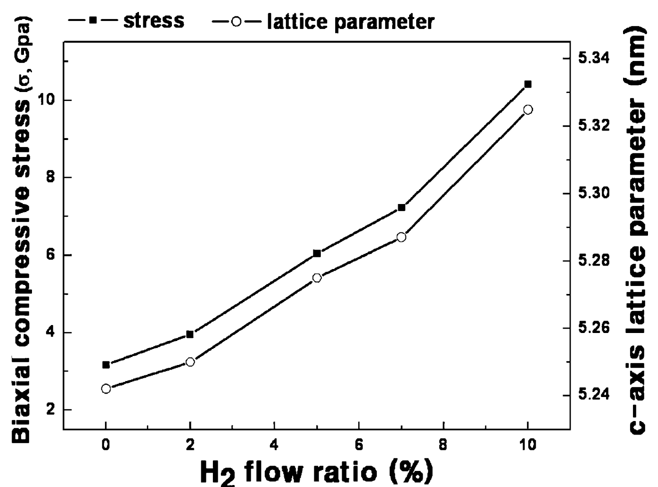

Fig. 3 X-ray diffraction measurements of intrinsic biaxial compressive stress and *c*-axis lattice parameter for AZO films deposited at different H_2 flow ratio

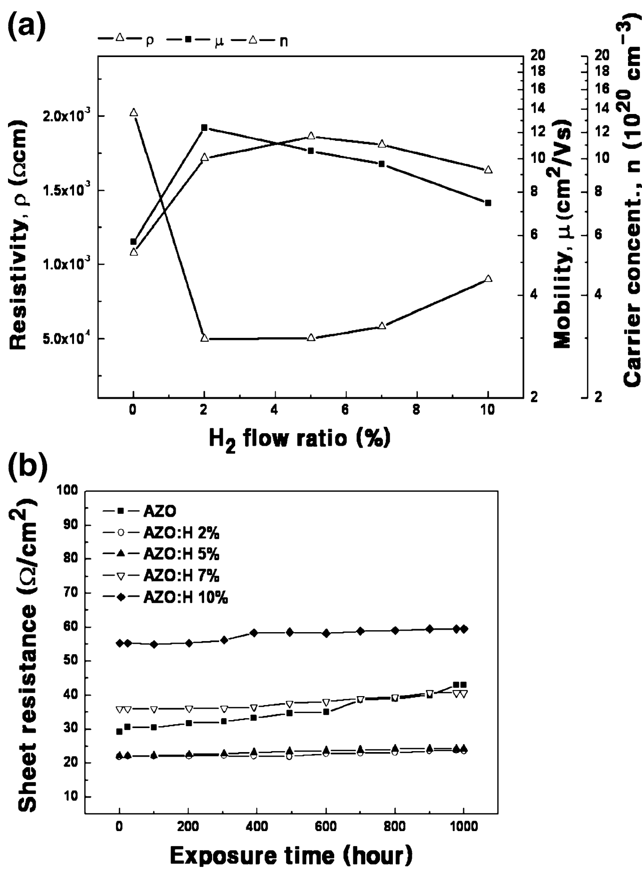

Fig. 4 (**a**) Resistivity, carrier concentration and mobility as a function of the H_2 flow ratio as determined by Hall measurement at room temperature. (**b**) Sheet resistance as a function of exposure time for AZO films prepared at various H_2 flow ratio

as well as the Hall mobility. The Hall mobility was highest for films deposited at H_2 flow ratio of 2%, then decreased gradually with increasing H_2 flow ratio. On the other hand, the carrier concentration reached maximum at H_2 flow ratio of 5%.

It has been shown that O–H (in H^+ form) stretch in Zn–O bond has the lowest formation energy, and that these hydrogens act as an n-type donor in ZnO related films [11]. Also, hydrogen can be incorporated into ZnO related films as an interstitial, and form dangling bonds at the grain boundaries. The increase in carrier concentration upon addition of hydrogen is thought to stem from the formation of O–H stretch inside Zn-O bond. Also increase of oxygen vacancies or Zn interstitials could be possible explanation for the increase of the carrier concentration. However, considering the large lattice expansion with increasing H_2 as shown in Fig. 3, the additional formation of oxygen vacancies due to hydrogen does not seem to be an appropriate explanation. The decrease in the Hall mobility with increasing H_2 suggests that the electron scattering is dominated by the ionized impurity. The irregular changes in the carrier concentration and the Hall mobility might be because hydrogen atoms located in the Zn–O bond center reach the H-doping saturated stage [11]. This suggests that hydrogen atoms exceed the H doping saturated stage, and many intergranular zinc atoms acting as electron donors are present in the films, which results in an increase in the carrier concentration. At the same time, intergranular zinc atoms form many scattering centers. The decrease in Hall mobility is due to these scattering centers. The substitutional complex consisting of oxygen vacancies and a hydrogen atom as well as interstitial hydrogen located between the O–Zn bonds shows a stable charged state, H^+. This is because only H^+ can have a stable charged state in ZnO, and the incorporated hydrogen atoms act as donors [11].

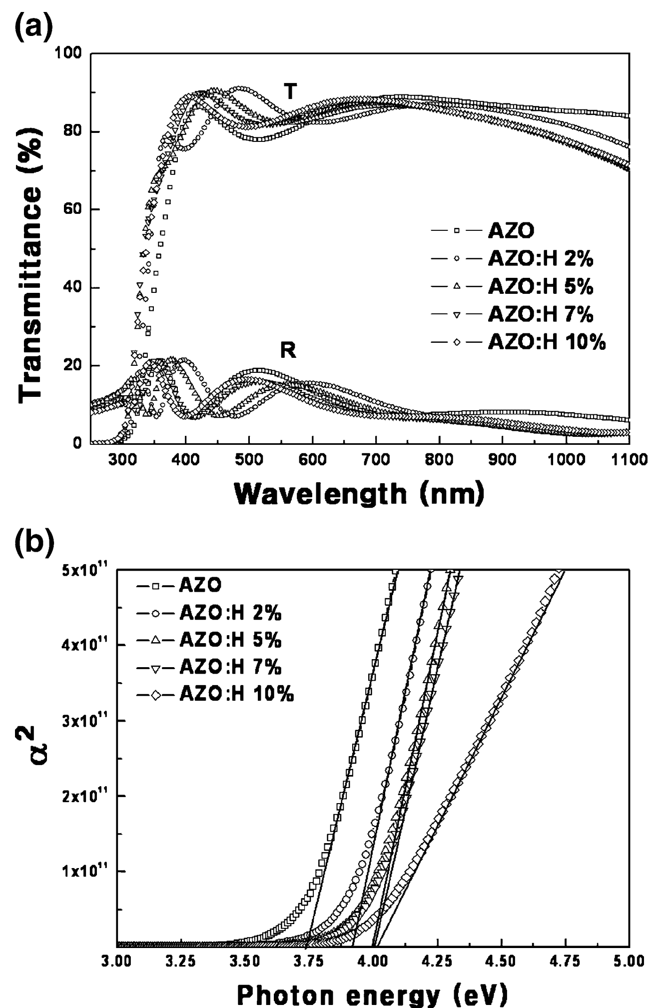

Fig. 5 (**a**) Transmittance and Reflectance spectra of Al doped ZnO in the wavelength 250–1,100 nm at different H_2 flow ratios. (**b**) Optical band-gap of Al doped ZnO at different H_2 flow ratios

Figure 4(b) shows the stability of the sheet resistance in the AZO and AZO/H films at room temperature under an air atmosphere. The sheet resistance of the non-hydrogenated AZO film increased monotonically with increasing exposure time due to the adsorption of oxygen at the surface and the grain boundaries, which will act as a trapping site of free carriers. On the other hand, AZO/H films showed remarkable improvement in the stability without any degradation. This result implies that certain portion of the hydrogen atoms incorporated in the AZO films are present at the grain boundaries, passivating the grain boundaries from the adsorption of oxygen species which would lead to a degradation of electrical properties.

Figure 5(a) shows the transmittance and reflectance spectra of the films sputtered under various H_2 flow ratios. The average optical transmittance in the visible light wavelength range was >85% that of the glass substrate for all samples. The average optical transmittance increased from 84.38% to 85.90%, while the average optical reflectance decreased from 11.87% to 10.42% with H_2 flow ratio from 0% to 10%. Direct allowed band gap of AZO and AZO/H films were evaluated optically by using relation of $\alpha h\nu \propto \left(h\nu - E_g\right)^{1/2}$ (for $h\nu > E_g$), where α is the absorption coefficient, h is Planck's constant, ν is frequency, E_g is band gap. The optical band gaps of films were estimated by plotting $(\alpha h\nu)^2$ vs. $h\nu$ and extrapolating the linear portion near the onset of absorption edge to the energy axis, as plotted in Fig. 5(b). The optical band gaps of AZO and AZO/H films were larger than that of the undoped ZnO (3.30 eV), and increased from 3.73 to 4.05 eV with increasing carrier concentration, which is due to band-filling effect known as Burstein–Moss shift.

In Fig. 6, the results obtained from the real-time measurement of resistance change during the heating and cooling cycle in ambient by using hot probe system (HPS) are shown. HPS enables real time measurements of the changes in the sheet resistance by heating or cooling under ambient conditions. The sample was heated to 500°C at a rate of 10°C/min, and then held at 500°C for 1 h. Finally, the samples were naturally cooled to RT. Although large initial resistances were obtained due to the contact resistance between a probe and thin film, the changes in the electrical properties of test samples were shown well. Non-hydrogenated AZO thin films showed a little change during heat treatment. But hydrogenated AZO films showed much larger increase in resistance upon thermal cycling, resulting in poorer thermal stability. It is notable that the onset of rapid resistance increase upon heating moved to lower temperature with increasing hydrogen content in sputter gas. Since the diffusion energy for hydrogen interstitials is known to be very small, being 0.9 eV, the hydrogen interstitials and the hydrogen atoms formed dangling bonds at the grain boundaries will be removed predominantly at the early stage

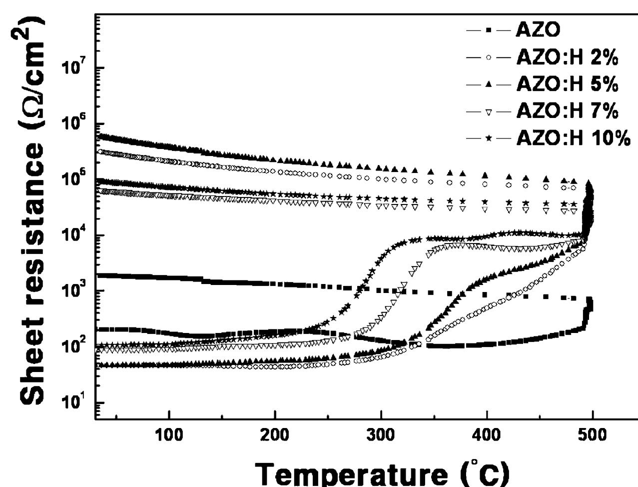

Fig. 6 Sheet resistance change of AZO and hydrogenated AZO films with respect to heat treatment temperature in air

of heating, and then isolated hydrogen at Zn–O bond will be removed [20]. AZO/H films deposited at higher H_2 possess larger grain boundaries due to smaller grains, leading to faster and larger evolution of hydrogen atoms at the early stage of heating. This result should be owed to a decrease of the hydrogen effect mentioned in a former chapter and an increase in the sheet resistance by the removal of activated hydrogen ions by heat treatment. The sheet resistance of hydrogenised AZO thin films started to increase at 250°C, and the changes in the sheet resistance increased with an increase of H_2 flow ratio.

The beneficial effect of hydrogen addition can be seen more clearly by considering the figure of merit (FOM), which is defined as the ratio of the electrical conductivity to the absorption coefficient averaged in visible range of 400–800 nm. The FOM of non-hydrogenated AZO film was 0.27 Ω^{-1}, but rose to 1.79 and 1.54 Ω^{-1} for AZO/H film deposited at H_2 flow ratio of 2% and 5%, respectively. The FOM decreased with further increase of H_2, but still remained larger than 1 Ω^{-1} even for film deposited at H_2 flow ratio 10%.

4 Conclusions

AZO thin films with a low resistivity and high transmittance were deposited by rf magnetron sputtering using a ZnO target mixed with 2 wt.% Al_2O_3 in Ar+H_2 ambient. All thin films exhibit a strong (002) c-axis oriented normal to the substrate. These results showed that H_2 has a strong influence on the properties of AZO films prepared at room temperature. The electrical, optical and structural properties of the AZO films prepared with different H_2 flow ratios showed variations related to the different H-doping state.

The optimal H_2 flow ratio range for preparing low resistivity and high transmittance AZO films was 2% to 5%. It is, therefore, suggested that the method presented in this study would be an effective way of modifying the electrical properties of hydrogenated Al-doped ZnO films that can be applied to device fabrication process with relative ease.

Acknowledgement This work is outcome of the fostering project of the Best Lab supported financially by the Ministry of Commerce, Industry and Energy (MOCIE)

References

1. B.Y. Oh, M.C. Jeong, W. Lee, J.M. Myoung, J. Cryst. Growth **274**, 453 (2005). doi:10.1016/j.jcrysgro.2004.10.026
2. A. Nuruddin, J.R. Abelson, Thin Solid Films **394**, 49 (2001). doi:10.1016/S0040-6090(01)01167-1
3. J.F. Wager, Science **300**, 1245 (2003). doi:10.1126/science.1085276
4. B.J. Ingram, G.B. Gonzalez, D.R. Kammler, M.I. Bertoni, T.O. Mason, J. Electroceram **13**, 167 (2004). doi:10.1007/s10832-004-5094-y
5. W. Wendt, K. Ellmer, K. Wiesemann, J. Appl. Phys **82**, 2115 (1997). doi:10.1063/1.366092
6. K. Yim, H. Kim, C. Lee, J. Electroceram **17**, 875 (2006). doi:10.1007/s10832-006-7036-3
7. Y. Igasaki, H. Saito, J. Appl. Phys **69**, 2190 (1991). doi:10.1063/1.348748
8. T. Tsuji, M. Hirohashi, Appl. Surf. Sci **157**, 47 (2000). doi:10.1016/S0169-4332(99)00517-6
9. S.A. Studenikin, N. Golego, M. Cocivera, J. Appl. Phys **87**, 2413 (2000). doi:10.1063/1.372194
10. J.F. Chang, W.C. Lin, M.H. Hon, Appl. Surf. Sci **183**, 18 (2001). doi:10.1016/S0169-4332(01)00541-4
11. C.G. Van de Walle, Phys. Rev. Lett. **85**, 1012 (2000). doi:10.1103/PhysRevLett.85.1012
12. R.J. Hong, K. Helming, X. Jiang, B. Szyszka, Appl. Surf. Sci. **226**, 378 (2004). doi:10.1016/j.apsusc.2003.10.040
13. Z.C. Jin, I. Hamberg, J. Appl. Phys **64**, 5117 (1988). doi:10.1063/1.342419
14. G. Sanon, R. Rip, A. Mansingh, Thin Solid Films 190, 287 (1990). doi:10.1016/0040-6090(89)90918-8
15. K. Zhang, A.R. Forouhi, I. Bloomer, J. Vac. Sci. Technol. A **17**, 1843 (1999). doi:10.1116/1.581902
16. A. Segmuller, M. Murakami, Analytical techniques for thin films (Academic, Boston, 1988), p. 143
17. K.H. Hellwege, A.M. Hellwege, Numerical data and functional relationships in science and technology, vol. 2 (Springer, Berlin, 1946) p. 58.
18. M.K. Puchert, P.Y. Timbrell, R.N. Lamb, J. Vac. Sci. Technol. A **14**, 2220 (1996). doi:10.1116/1.580050
19. M.K. Hudiat, P. Modak, S.B. Krupanidhi, Mater. Sci. Eng. B **60** (1), 11 (1999)
20. E.V. Lavrov, J. Weber, F. Borrnert, C.G. Van de Walle, R. Helbig, Phys. Rev. B **66**, 165205 (2002). doi:10.1103/PhysRevB.66.165205